

RESEARCH ARTICLE

A generalized printing process window for preventing surface overcuring in volumetric additive manufacturing

Supplementary File

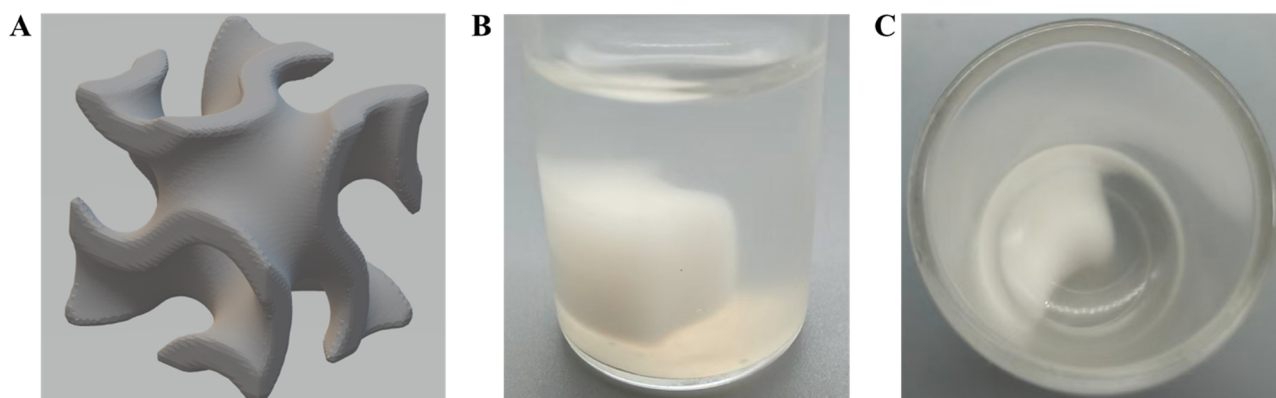


Figure S1. Demonstration of severe surface overcuring defect during the volumetric additive manufacturing of a complex geometry. (A) The target computer-aided design model of a triply periodic minimal surface structure. (B, C) Photographs of the failed print (F5 ink, $A \approx 1.23$, $r \approx 3.5$ mm) from different viewing angles. As shown, the intricate structural features are completely obscured by the amorphous overcured resin adhering to the vat wall.

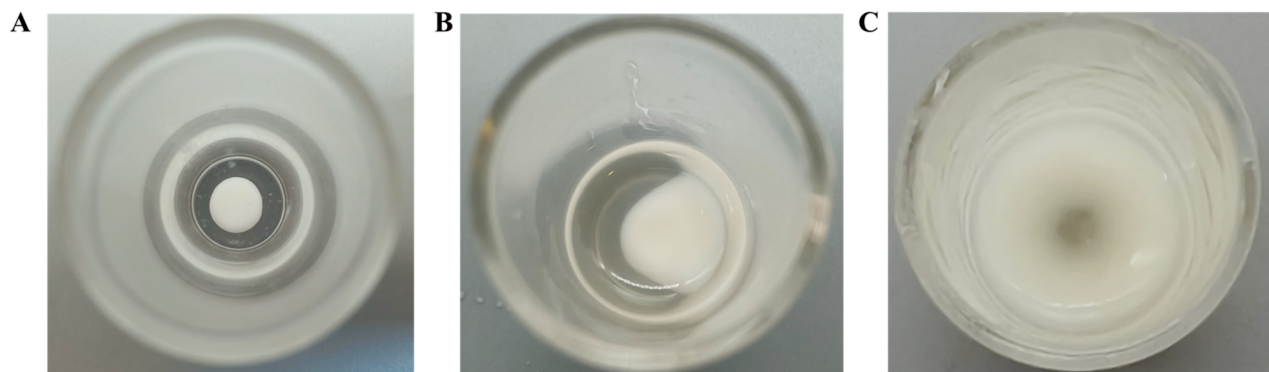


Figure S2. High-resolution photographs corresponding to the insets in Figure 2A of the paper. These images detail the distinct morphological differences between (A) a successful volumetric print fabricated within the optimal process window, and (B, C) failed prints characterized by severe surface overcuring and subsequent vat wall adhesion.

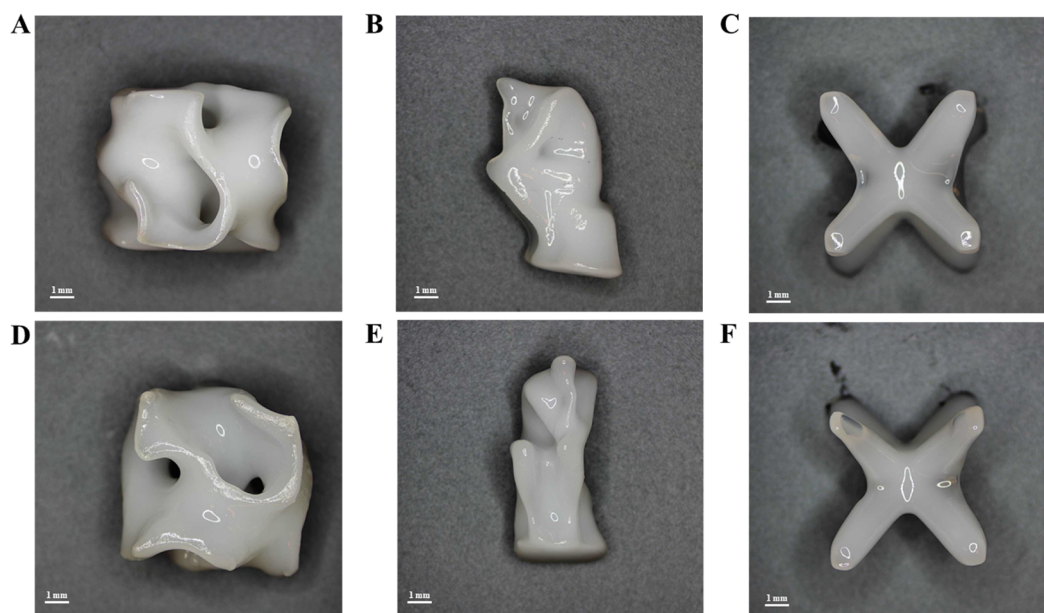


Figure S3. Photographs of the printed complex geometries: (A, D) Triply periodic minimal surface, (B, E) The Thinker, and (C, F) body-centered cubic from different viewing angles. Scale bars: 1 mm.

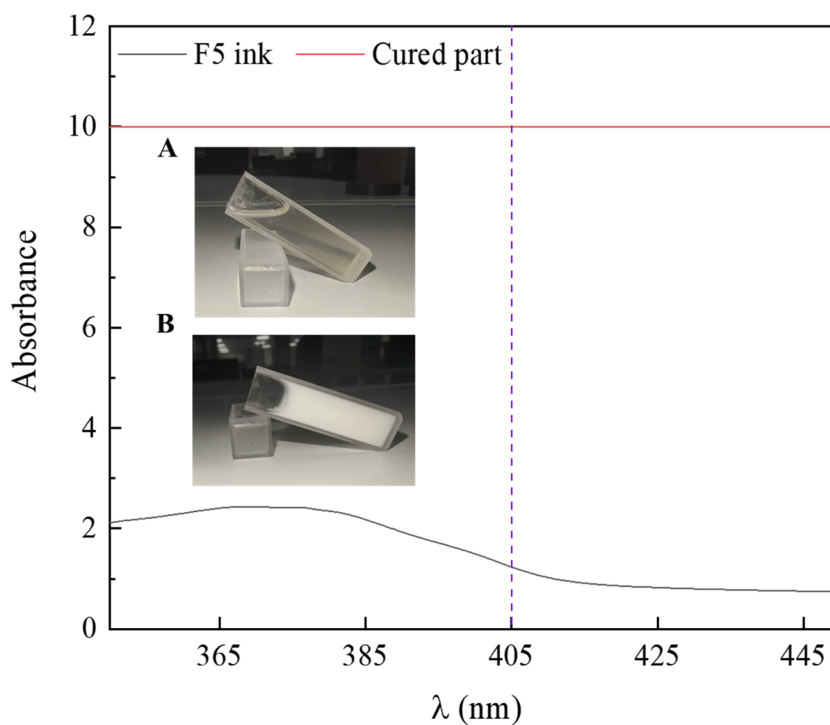


Figure S4. Comparative optical absorbance spectra of the F5 formulation in liquid and cured states (measured using standard 1 cm cuvettes via a Lambda 1050+ spectrophotometer). The transition from a liquid ink to a solid hydrogel induces a dramatic increase in absorbance to the instrumental limit ($A \geq 10$), effectively rendering the cured part an optically opaque medium for multi-material overprinting. Insets show photographs of the F5 ink (A) before and (B) after curing, respectively.

Table S1. Literature-reported process parameters for VAM

References	Ink	Absorbance	Inner radius of the vat	Maximum radius of the print
Xie <i>et al.</i> ¹	Silk-based (bio)ink	~0.17	~6.0 mm	~3.0 mm
Behravesht <i>et al.</i> ²	Resin from Anycubic	~0.77	~6.0 mm	~4.0 mm
Bernal <i>et al.</i> ³	GelMA	~0.26	~8.9 mm	~7.0 mm
Kollep <i>et al.</i> ⁴	Polysiloxane ceramic precursor	~0.80	~8.2 mm	~5.0 mm
Madrid-Wolff <i>et al.</i> ⁵	Acrylic resin with TiO ₂ nanoparticles	~0.58	~8.0 mm	~5.0 mm
Chen <i>et al.</i> ⁶	Acrylic resin	~1.00	~10.0 mm	~5.0 mm
Ribezzi <i>et al.</i> ⁷	GelMA	~0.20	~6.6 mm	~5.3 mm
Ribezzi <i>et al.</i> ⁷	GelMA	~0.20	~6.6 mm	~4.0 mm (z ≈ 2.2 mm)
Pellizzon <i>et al.</i> ⁸	GelMA	~0.15	~8.0 mm	~5.8 mm (z ≈ 2.6 mm)

Abbreviations: GelMA: Gelatin methacryloyl; TiO₂: Titanium dioxide; VAM: Volumetric additive manufacturing.

Table S2. Measured dimensions of the printed structures

Dimension (mm)	TPMS	The Thinker	BCC
X	7.75 ± 0.29 (7.5)	5.86 ± 0.06 (6.0)	6.44 ± 0.12 (6.5)
Y	7.65 ± 0.34 (7.5)	3.86 ± 0.06 (4.0)	6.62 ± 0.12 (6.5)
Z	6.88 ± 0.10 (7.0)	8.25 ± 0.08 (8.0)	6.76 ± 0.07 (6.5)
Wall thickness	0.62 ± 0.11 (0.5)	–	1.38 ± 0.13 (1.0)

Notes: The values enclosed in parentheses represent the design dimensions of the printed parts, whereas the others represent the measured dimensions. All data were calculated using at least three samples.

Abbreviations: BCC: Body-centered cubic; TPMS: Triply periodic minimal surface.

References

- Xie M, Lian L, Mu X, *et al.* Volumetric additive manufacturing of pristine silk-based (bio)inks. *Nat Commun.* 2023;14(1):210. doi: 10.1038/s41467-023-35807-7
- Behravesht AH, Tariq A, Buni J, Rizvi G. Computed tomography-based volumetric additive manufacturing: Development of a model based on resin properties and part size interrelationship—Part I. *J Manuf Mater Process.* 2025;9(6):178. doi: 10.3390/jmmp9060178
- Bernal PN, Delrot P, Loterie D, *et al.* Volumetric bioprinting of complex living-tissue constructs within seconds. *Adv Mater.* 2019;31(42):1904209. doi: 10.1002/adma.201904209
- Kollep M, Konstantinou G, Madrid-Wolff J, *et al.* Tomographic volumetric additive manufacturing of silicon oxycarbide ceramics. *Adv Eng Mater.* 2022;24(7):2101345. doi: 10.1002/adem.202101345
- Madrid-Wolff J, Boniface A, Loterie D, Delrot P, Moser C. Controlling light in scattering materials for volumetric additive manufacturing. *Adv Sci.* 2022;9(22):2105144. doi: 10.1002/advs.202105144
- Chen T, You S, Xu L, *et al.* High-fidelity tomographic additive manufacturing for large-volume and high-attenuation situations using expectation maximization algorithm. *Addit Manuf.* 2024;80:103968. doi: 10.1016/j.addma.2024.103968
- Ribezzi D, Gueye M, Florczak S, *et al.* Shaping synthetic multicellular and complex multi-material tissues via embedded extrusion-volumetric printing of microgels. *Adv Mater.* 2023;35(36):2301673. doi: 10.1002/adma.202301673
- Pellizzon N, Šeta B, Kruse CS, Salajeghe R, Spangenberg J. Investigating thermal strains and chemical shrinkage in tomographic volumetric additive manufacturing. *Addit Manuf.* 2025;105:104781. doi: 10.1016/j.addma.2025.104781